VOLUME 2

DISEASE CONTROL PRIORITIES • FOURTH EDITION

Investing in Pandemic Prevention, Preparedness, and Response

Chapter 2 Annexes

ANNEX 2A. TECHNICAL SUPPLEMENT

The epidemic risk modeling framework developed to produce the estimates in this chapter draws upon principles from computational epidemiology, social science, economics, actuarial science, risk management, and extreme events modeling. It includes a disease spread model, development of exceedance probability (EP) curves, and estimation of the expected mortality. This annex provides detailed methods for each of these components.

The disease spread model used here is a disease-specific, stochastic, global, metapopulation, compartmental model that simulates the daily spatio-temporal progression of disease spread. It includes mechanistic modeling of underreporting to correct for uncertainty in reported infectious disease statistics and incorporates an Epidemic Preparedness Index to model likely intervention scenarios and how they may differ for 200+ countries and territories (Oppenheim et al. 2019). It also includes response measures.

For each simulation within the event catalog, plausible model input parameters and initial conditions were derived from analyses of historical data and scientific literature. The simulations incorporate epidemiologic knowledge of pathogens and population characteristics that can affect transmission dynamics and the likelihood of severe outcomes.

The model included pandemic influenza and epidemic/novel coronaviruses to represent a catalog of epidemics and pandemics caused by respiratory pathogens having high pandemic potential. These catalogs included events caused by novel, human-to-human transmissible influenza A viruses and novel viruses in the subfamily Orthocoronavirinae that are zoonotic in origin and cause disease in humans, such as SARS-CoV-1, MERS-CoV, and SARS-CoV-2.[1] Seasonal and endemic diseases, such as seasonal influenza and seasonal coronaviruses (which typically cause mild disease in humans), were considered to be part of the "baseline risk," which is adequately represented in historical mortality data, and thus were not included.

The output of the risk model is a modeled event catalog (table 2.1 in the main text), a database containing many hypothetical views of the potential loss that may be experienced in a given year (Madhav et al. 2017; Madhav, Stephenson, and Oppenheim 2021). The event catalog serves as a basis for probabilistic estimation of potential human and economic losses caused by epidemics, and was used to analyze the frequency and severity of infectious disease epidemics caused by respiratory pathogens of concern.

The event catalogs were generated using simulations produced by the disease spread model described earlier. Simulations are initiated with parameter values sampled from probability distributions. Parameters are instead held constant if they are relatively invariant across observed epidemics, are not influential to the model outcomes, or do not have sufficient historic data to develop a probability distribution. With the sampling approach, the most probable parameter values

are represented more often in the event catalog, and the extreme values for that parameter will rarely occur. The outcome of this process is an event catalog that captures the probabilities of the occurrence of different-magnitude events in any given year.

The frequency of events is a key driver of overall epidemic risk. The modeled event frequency is characterized either by the time between events in the historical record (that is, interarrival time) or, for more frequently occurring events, the number of epidemics per year. For pathogens that are rare, many simulated years in the event catalog do not contain any epidemics, whereas catalogs for more frequent events may contain more than one event per year.

Disease Spread Model

A key component of the risk modeling framework is a computational epidemiology-based disease spread model. The disease spread model begins with zoonotic disease spillover from an animal host and simulates human-to-human disease transmission between and within thousands of modeled geographic subpopulations across the world. The model framework consists of a stochastic, metapopulation compartment model coupled with human mobility networks overlaid across a human population layer, with underpinnings comparable to previously published models (Balcan et al. 2009; Colizza et al. 2007) and including the following enhancements.

Population layer. The disease spread models used here originally operated over a global human population layer constructed from available census data and United Nations estimates (UN DESA 2015). As described in the main text, the model was subsequently updated to include more recent population data (UN DESA 2022). Individuals are partitioned into subpopulations that correspond to administrative subdivisions. During simulations, individuals are assumed to interact homogeneously within each subpopulation. Disease is transmitted between and within each subpopulation on a daily time step.

Mobility model. Outbreaks spread locally within subpopulations as people interact with their communities, and across the globe through long-distance travel. In the disease spread model, pathogens spread between subpopulations through mobility networks. Long-range mobility (air travel) occurs on a daily time scale. Short-range mobility (daily commuting) occurs over a time period shorter than one day. Rapid human movement via air travel facilitates global epidemic spread. Air travel is incorporated into the disease spread model by probabilistically moving individuals between geographic subpopulations according to domestic and international air traffic data. Air traffic data, consisting of the number of individuals who travel between each airport, were used to calculate the daily probability of air travel between connected subpopulations.[2] Each individual in an epidemiological model compartment that has the ability to travel (based on disease status) has the potential to move to a connected subpopulation every simulation day, resulting in minor changes to the number of individuals in each subpopulation over time.

The model also includes short-range mobility, which estimates the daily probability that an individual travels between two adjacent subpopulations. The short-range mobility model assumes that individuals who commute for work generally spend one-third of the day in their destination location and spend the remainder of the time in their origin location. This general assumption reflects the average amount of time persons spend at work during a day. The proportion of the population that commutes each day is estimated at the country level based on the labor force, unemployment, and road networks.

Epidemic Preparedness Index (EPI). Epidemic preparedness and response capacity are important factors that influence outbreak severity. The EPI is a comprehensive metric used in the disease spread models to capture the geographic variation in outbreak preparedness and response capacity. It reflects the geographic subpopulation's ability to detect and respond to an epidemic event, with scores ranging from 0 (least prepared) to 100 (most prepared) (Oppenheim et al. 2019).

Reporting bias. Real-world observational outbreak data are always affected by reporting biases because not all information is known or reported to health authorities, especially in real time (Dalziel et al. 2018; Gamado, Streftaris, and Zachary 2017). Reporting biases are notably present especially before the causative agent of the outbreak is known. The disease spread model output must be interpreted in light of reporting biases for comparison with real-world outbreak data. A model that estimates a pathogen-specific reporting rate at the national level was built to address this issue. The estimated reporting rate from this model is used in the compartment model to more closely reflect the real number of cases. Development of this model involved collection of pathogen- and country-specific reporting rates from the scientific literature along with potential predictor variables that can be used to inform the model (Meadows et al. 2022).

Epidemiological compartment model. To simulate disease spread, the epidemiologic model compartmentalizes human subpopulations by disease state. An individual can exist in only one disease state at any given time. The model probabilistically captures the progression of individuals through each disease state using a series of transition rates. Stochastic transitions between model compartments capture the inherent variation in disease transmission and progression. Compartment transitions are defined by discrete stochastic chain binomial and multinomial processes. The model calculates the number of individuals in each disease state by geographic subpopulation for each simulation day.

The epidemic model uses a specialized SEIHR (Susceptible–Exposed–Infectious–Hospitalized–Recovered) compartmental structure (figure 2A.1). The ability to travel or commute and infect other individuals is defined for each compartment (table 2A.1). Infectious individuals can spread disease within their subpopulation and to other geographic subpopulations if the individuals travel. Mass vaccination campaigns are also explicitly incorporated into the compartment model structure.

Figure 2A.1 Epidemiological Compartment Model

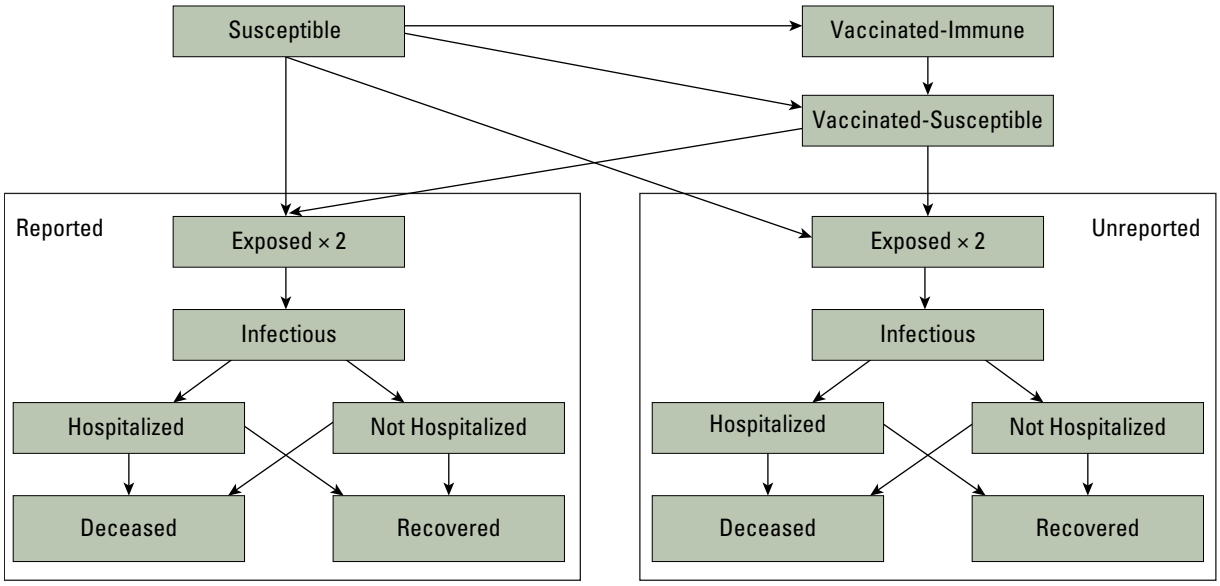

Source: Original figure created for this publication.

At the start of the event, all individuals are in the Susceptible compartment and a single individual is added to the Exposed compartment. The simulation continues until no individuals are in the Exposed, Infectious, Hospitalized, or Not-Hospitalized compartments. Long- and short-distance travel is explicitly modeled for Exposed and Infectious compartments. Individuals in the Hospitalized, Not-Hospitalized, and Deceased compartments are assumed to not travel. Air travel of Susceptible, Recovered, and Vaccinated compartments is not modeled because these compartments do not contribute to the movement of infection (table 2A.1).

The modeled transition rate from the Susceptible to the Exposed state is determined by the force of infection (FOI). Exposed individuals progress through two sequential Exposed compartments so that the duration of the incubation period is Erlang-distributed. At this stage individuals are then assigned to Reported or Unreported status based on the reporting ratio. They then progress into the Infectious compartments at a daily rate, epsilon, the inverse of the average incubation period.

Individuals in the Infectious compartments may then transition into the Hospitalized or Not-Hospitalized states at a daily rate, gamma. This rate is associated with the average time between symptom onset and health care use; however, the model also includes a Not-Hospitalized compartment that captures individuals not cared for in a traditional hospital setting. Individuals in these two compartments cannot travel. Individuals in the Hospitalized and Not-Hospitalized compartments then move into the Recovered or Deceased state at a daily rate, mu, based on the average time to recovery or death and case fatality ratio. Table 2A.2 shows transition rates.

Table 2A.1 Description of Modeled Disease States, Their Infectivity, and Their Ability to Commute

State	Description	Mobility	Infectious
Susceptible	Individuals susceptible to infection	Yes[a]	No
Exposed 1 and 2	Individuals exposed to disease, not yet infectious	Yes	No
Infectious	Infected and showing symptoms	Yes	Yes
Not Hospitalized	Infected individuals who are not treated in a traditional hospital setting	No	Yes
Hospitalized	Infected individuals who are hospitalized	No	Yes
Recovered	Individuals who have recovered from infection and are now immune	Yes[a]	No
Deceased	Individuals who have died of their infection and are not infectious	No	No
Vaccinated-Immune	Individuals who are vaccinated and become immune to future infection	Yes[a]	No
Vaccinated-Susceptible	Individuals who are vaccinated but do not achieve immunity and remain susceptible to future infection	Yes[a]	No

Source: Original table created for this publication.

Note: Mobility indicates whether or not individuals in the state are incorporated into the long- and short-range mobility networks.

a. Because of computational constraints, Susceptible, Recovered, and Vaccinated individuals are incorporated only into short-range (not long-range) mobility networks.

Table 2A.2 Description of Model Transition Rates

Transition	Transition rates
Susceptible → Exposed 1	FOI
Exposed 1 → Exposed 2 – Reported	epsilon / 2 * RR
Exposed 1 → Exposed 2 – Unreported	epsilon / 2 * (1 – RR)
Exposed 2 → Infectious	(epsilon / 2)
Infectious → Hospitalized	gamma * CHR
Infectious → Not Hospitalized	gamma * (1 – CHR)
Hospitalized or Not Hospitalized → Recovered	mu * (1 – CFR)
Hospitalized or Not Hospitalized → Deceased	mu * CFR
Susceptible → Vaccinated - Immune[a]	VxRate * VxEff
Susceptible → Vaccinated - Susceptible [a]	VxRate * (1 – VxEff)

Source: Original table created for this publication.

Note: CFR = case fatality ratio; CHR = case hospitalization ratio; FOI = force of infection; RR = reporting ratio; VxRate = vaccination rate; VxEff = vaccination efficacy.

a. Transitions from the Susceptible compartment to the Vaccinated-Immune and Vaccinated-Susceptible compartments occur only after the vaccine start day and continue until the maximum proportion of the population to be vaccinated is achieved.

The FOI, as shown in equation (2A.1) dictates the rate of transition from Susceptible to Exposed and is based on the reproduction number (R_t), the infectious period (1/gamma), the total number of infectious individuals in the subpopulation, and the total number of individuals in the subpopulation (N_i). FOI is calculated for each subpopulation, *i*, on each day, *t*, using the equation:

$$FOI_{i,t} = \frac{R_t}{(1/gamma)} * \frac{(Total\ Infectious)_i}{N_i} \quad (2A.1)$$

Model Parameterization

Model parameter distributions are estimated through review and analysis of the scientific literature and historical data, including from prior events and modeling studies (table 2A.3). The fitted distributions may be parametric or nonparametric, discrete or continuous, as warranted by the data and biological plausibility. Figure 2A.2 shows the process of distribution fitting and assessment.

Table 2A.3 Model Parameter Types and Ranges of Values

Parameter	Pandemic influenza	MERS-like coronaviruses	SARS-like coronaviruses
R_0 (basic reproduction number)	Nonparametric (refer to following table) (min = 1.00, max = 3.00) R_0 range / Relative frequency (%) 1.00–1.30 / 0.13 1.31–1.50 / 1.69 1.51–1.70 / 7.00 1.71–1.90 / 25.98 1.91–2.10 / 46.92 2.11–2.30 / 12.28 2.31–3.00 / 6.00 Also varies by season. (Balcan et al. 2009; Jackson, Vynnycky, and Mangtani 2010; Longini et al. 2005; Rizzo et al. 2011; Tuite et al. 2010; White et al. 2009; White and Pagano 2008; Yang et al. 2009; Zhang et al. 2009)	Triangular (min = 0.5, max = 0.9, mode = 0.7) (Breban, Riou, and Fontanet 2013; Cauchemez et al. 2014)	Triangular (min = 0.5, max = 2.8, mode = 1.2) (Adam et al. 2020; Chowell et al. 2015; Lipsitch et al. 2003)
K (superspreading dispersion parameter)	None	Uniform (min = 0.05, max = 0.10) (Choe, Kim, and Lee 2020)	Uniform (min = 0.35, max = 0.45) (Adam et al. 2020; Lau et al. 2020)
Incubation period (days)	Non-parametric (min = 1, max = 4) (Lessler et al. 2009; WHO 2009)	Truncated Lognormal (min = 1, max = 14) (Cauchemez et al. 2014)	Gamma (min = 1, max = 6) (Alene et al. 2021; McAloon et al. 2020)
Infectious period	Lognormal (min = 2, max = 5) (Carrat et al. 2008; Longini et al. 2005; Rvachev and Longini 1985; Tizzoni et al. 2012; Tuite et al. 2010)	Fixed value (value = 5.2) (Cauchemez et al. 2014)	Fixed value (value = 5.2) (Cauchemez et al. 2014)

Sources: As indicated in the table.

Note: MERS = Middle East respiratory syndrome; SARS = severe acute respiratory syndrome.

Figure 2A.2 Process for Fitting Model Parameter Distributions

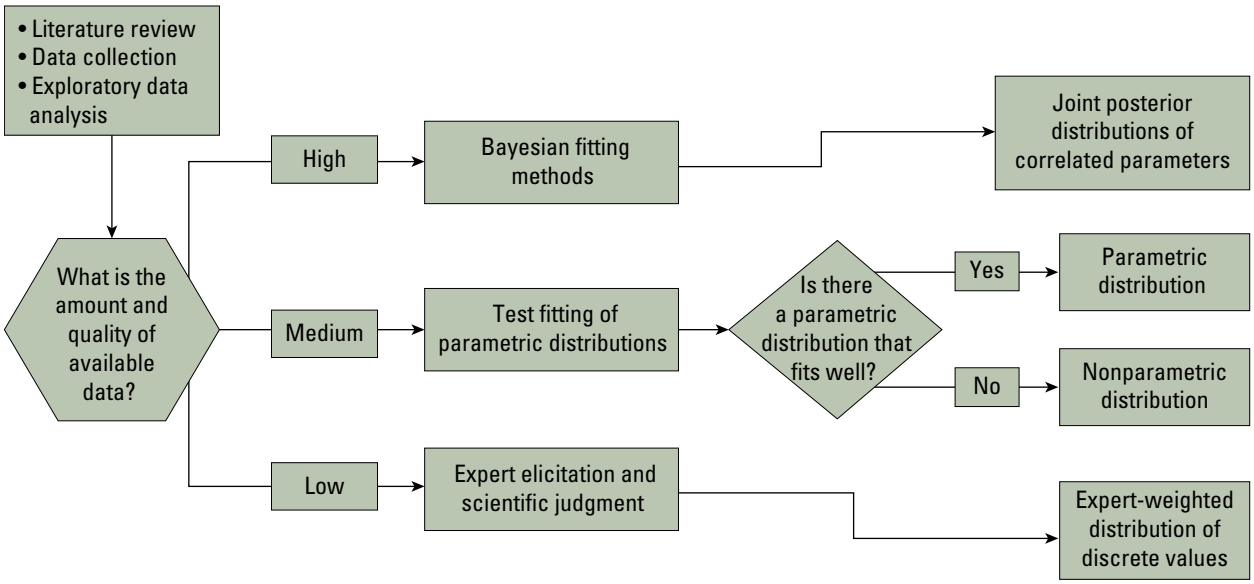

Source: Original figure created for this publication.

Model parameters have varying levels of available data from historical events and the scientific literature that would allow for fitting of statistical distributions. There may be several reasons why parameters are less well-represented in the historical record and scientific literature, including a lack of historical events, lack of published data, or a lack of interest from the scientific community in estimating a particular parameter.

Transmissibility, whose initial value in the model is represented by R_0, is influenced by pathogen characteristics, host characteristics, and population/environmental characteristics, including population density, social interaction, and sanitation practices. The R_0 parameter is well-characterized in the scientific literature for several pathogens because of the strong scientific and public health interest in understanding the transmissibility of pathogens. Infectious period is also well-represented in the scientific literature, although not as represented as R_0 because most methodologies for estimating infectious periods require clinical observations or viral shedding studies, whereas R_0 can be estimated solely from case counts over time, which are more likely to be publicly reported.

Intervention and Response Measures

Epidemic preparedness and response are critical determinants of event trajectory. The complexities of outbreak preparedness and response are captured in the disease spread model through a series of intervention parameters that capture activities that result in the reduction in the disease transmission rate, such as infection control improvements and social distancing. Model parameters pertaining to interventions are highlighted in table 2A.4, with distributions and ranges shown in table 2A.5.

Table 2A.4 Model Parameters Associated with Interventions and Vaccination

Parameter	Description
Vaccination rate	Proportion of the susceptible population that is vaccinated per day
Vaccine efficacy	If a vaccine is available, the proportion of vaccinated individuals who become immune to infection
Vaccine proportion	If a vaccine is available, the maximum proportion of the population that is vaccinated
Vaccine deployment time	If a vaccine is available, the time between the start of the event and vaccine deployment
Intervention time	The time between the start of the event and attempt at outbreak containment
Intervention R_t	The effective reproduction number after intervention

Source: Original table created for this publication.

Table 2A.5 Intervention and Outcome Parameter Distributions and Ranges

Parameter	Pandemic influenza	MERS-like coronaviruses	SARS-like coronaviruses
CHR	Nonparametric (min = 0.0004, max = 0.4) (Andreasen, Viboud, and Simonsen 2008; Chowell et al. 2011; Gani et al. 2005; Presanis et al. 2009; Shrestha et al. 2011; Shubin et al. 2014; Wu et al. 2010)	Triangular (min = 0.95, max = 1) (Rivers et al. 2016)	Function of CFR (Angulo, Finelli, and Swerdlow 2021)
CFR (also varies by EPI quintile and age)	Pareto (shape = 2.166573859, scale = 0.001450627) (min = 0.00017, max = 0.29) (Britten 1932; Lee et al. 2008; Valleron et al. 2010; Wong et al. 2013)	Triangular (min = 0.3, max = 0.4, mode = 0.35) (Majumder et al. 2014; Rivers, Majumder, and Lofgren 2016)[a]	Beta (shape1 = 0.5, shape2 = 35) (min = 0, max = 0.24) (Grewelle and Leo 2020; Jia et al. 2009; Kenyon 2020; Liang et al. 2007; Luo et al. 2021)[b]
Vaccination rate (proportion of population per day)	Uniform (min = 0.045%, max = 1.1%) (Henderson et al. 2009; Mihigo et al. 2012; Tizzoni et al. 2012; WHO 2013)	None (Tai et al. 2022)	Gamma (min = 0%, max = 4.2%) Varies by EPI quintile (Mathieu et al. 2020)
Vaccine efficacy	Discrete (min = 0.60, max = 0.80) (Longini et al. 2004)	None (Tai et al. 2022)	Uniform (min = 0.5, max = 0.8) (Graña et al. 2023)
Vaccine proportion	Based on CHR, varies by country (Mihigo et al. 2012; Tizzoni et al. 2012; WHO 2013)	None (Tai et al. 2022)	Uniform (min = 0.5, max = 0.8) (Mathieu et al. 2020)
Vaccine deployment time (start day)	Discrete (min = 180, max= ∞) Varies by EPI quintile (Hessel and EVM Influenza Working Group 2009; WHO 2013)	None (Tai et al. 2022)	Uniform (min = 120, max = 600) Varies by EPI quintile (Mathieu et al. 2020)
Intervention time (weeks)	Discrete (min = 4, max = 12) (Martinez and Das 2014; Oppenheim et al. 2019)	Fixed value (value = 52) (Breban, Riou, and Fontanet 2013)	Uniform (min = 10, max = 32) (Ali et al. 2020)
Intervention R_t	R_0 reduction (min = 3%, max = 10%) Varies by EPI quintile (Martinez and Das 2014; Oppenheim et al. 2019)	Fixed value (value = 0.5) (Breban, Riou, and Fontanet 2013)	Decay over time (Ali et al. 2020; Chowell et al. 2004) Analysis of Ginkgo Biosecurity data set[c]

Source: As indicated in the table.

Note: CFR = case fatality ratio; CHR = case hospitalization ratio; EPI = Epidemic Preparedness Index; MERS = Middle East respiratory syndrome; SARS = severe acute respiratory syndrome.

a. Also, Andrew Rambaut, "MERS Cases," https://github.com/rambaut/MERS-Cases (retrieved April 3, 2017).

b. World Health Organization, "Summary of Probable SARS Cases with Onset of Illness from 1 November 2002 to 31 July 2003," http://www.who.int/csr/sars/country/table2004_04_21/en/.

c. Ginkgo Biosecurity, "Spatiotemporal Data for 2019-Novel Coronavirus Covid-19 Cases and Deaths," Humanitarian Data Exchange. https://data.humdata.org/dataset/2019-novel-coronavirus-cases.

Epidemic response strategies typically include pharmaceutical interventions and public health and social measures. Pharmaceutical interventions can reduce transmission by preventing infection or reducing pathogen shedding; alternatively, pharmaceutical interventions may reduce the case fatality ratio by improving patients' clinical course. Examples of pharmaceutical interventions include vaccines and therapeutics. Public health and social measures encompass efforts to reduce transmission, such as improved sanitation, social distancing, and reduced population mobility. Examples include masking, contact tracing, quarantine, isolation, or lockdowns, as occurred during COVID-19, and can also include mitigation of risks associated with cultural factors that play a role in transmission. Public health and social measures also include basic patient supportive care. The effectiveness of interventions depends heavily on social and political factors, such as the willingness of the public to comply with health regulations and adopt risk-reducing behavior. Therefore, effective risk communication and building population trust are critical aspects of epidemic response.

Epidemic control measures can include quarantine, isolation, strict infection control procedures in health care settings, antiviral therapies, and vaccination. Factors that determine the impacts of these control measures include time to deployment, available resources, and the ability to effectively communicate with the affected communities (Liu et al. 2015).

The infrequency of large-scale epidemics has resulted in a lack of information about how countries will respond. Additionally, these responses have changed significantly in the last few decades, making information from historic events less reliable. For example, during the 40 years spanning 1980 to 2020, only one influenza pandemic tested the public health system's ability to detect a novel influenza virus and create and distribute a new vaccine. For this reason, such parameters have greater uncertainty and rely to a greater extent on the elicitation of expert opinion and scientific judgment.

Vaccination campaigns. For respiratory pathogen outbreaks, mass vaccine campaigns are explicitly modeled using model parameters as described in tables 2A.4 and 2A.5. The probability of vaccination (when a vaccine is available) depends on these parameters.

The Vaccine Efficacy parameter indicates the proportion of vaccinated individuals who experience complete protection from the modeled virus infection (Nichol and Treanor 2006). Vaccine Efficacy is set to zero if vaccination resources are not available during the modeled scenario, although other interventions, which reduce transmission, still occur. This scenario represents the possibility of resource limitations preventing vaccination campaigns.

The number of vaccines available during an outbreak is represented by the Vaccine Proportion variable. This parameter is intended to reflect the potential challenges in production and provision of vaccinations as well as vaccine uptake by the population. Vaccine Proportion is applied in the model by tracking the number of doses administered. Once the Vaccine Proportion is reached, Vaccination Rate is set to zero.

The Vaccine Deployment Time varies by simulation. Before the Vaccine Deployment Time, the Vaccination Rate for all subpopulations is zero. Once Vaccine Deployment Time occurs, members of each subpopulation receive vaccine on a daily basis, according to Vaccination Rate parameter, which varies by EPI.

General intervention measures. In addition to vaccination campaigns, the model includes an overall reduction in transmissibility due to public health and social measures, which represents an attempt at containment. In the model, transmissibility after implementation of the intervention measures is described by the parameter, R_t (the effective reproduction number at time t) (Bo et al. 2021).

The Intervention Time parameter describes when transmission reduction starts to occur as a result of intervention measures. Because of the limited historical data on time to intervention, the model uses the time difference between the onset of the first case to the time of first report as a proxy measure for intervention time. Reporting timeliness has been used as a proxy measure in previous research to assess surveillance and response systems (Chan et al. 2010).

The preparedness and response capacity of a region, based on EPI, is assumed to affect the Intervention Time parameter. Intervention Time is represented by a negative binomial distribution for each subpopulation according to their EPI equal interval quantile category. The negative binomial distribution was derived by fitting the distribution to the number of days between the onset of the first case (as reported in any data source) and the date of first report by the World Health Organization Disease Outbreak News reports (Oppenheim et al. 2019). This analysis contains data from January 1996 through August 2018, and excludes events caused by toxin, chemical, foodborne, vector-borne, or unknown pathogens. Figure 2A.3 displays the empirical distribution of time to report by EPI quantile.

Figure 2A.3 Time to Report by Epidemic Preparedness Index (EPI) Equal Interval Quantile

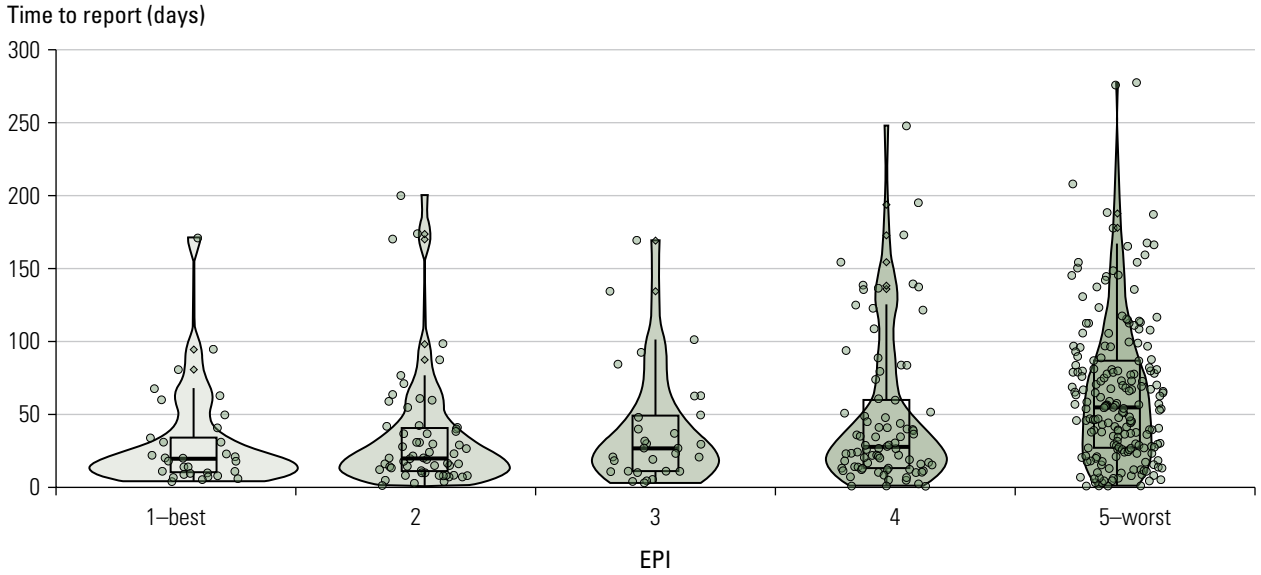

Source: Original figure created for this publication.

The value of R_t after interventions is based on the estimated efficacy of public health and social measures. Once a simulated event reaches the Intervention Time, the modeled transmissibility parameter is decreased linearly over the following two-week time period until R_t equals the new value. The R_t values are assumed based on observations from previous epidemics and modeling studies (Bo et al. 2021; Wu et al. 2006).

Outcomes Modeling

Hospitalizations are modeled using the case hospitalization ratio (CHR) distribution, estimated by analysis from scientific literature and available data. The CHR estimates the proportion of infected individuals who become ill enough to require and obtain hospital care.

Mortality is modeled according to the case fatality ratio (CFR) distribution, which is also estimated based on analysis of scientific literature and available data. The CFR represents the proportion of infected individuals who succumb to the illness.

There is strong evidence of correlation between CHR and CFR, which is incorporated into the model (figure 2A.4). Table 2A.5 shows the assumed distributions of CHR and CFR.

Figure 2A.4 Modeled Relationship between Case Fatality Ratio (CFR) and Case Hospitalization Ratio (CHR)

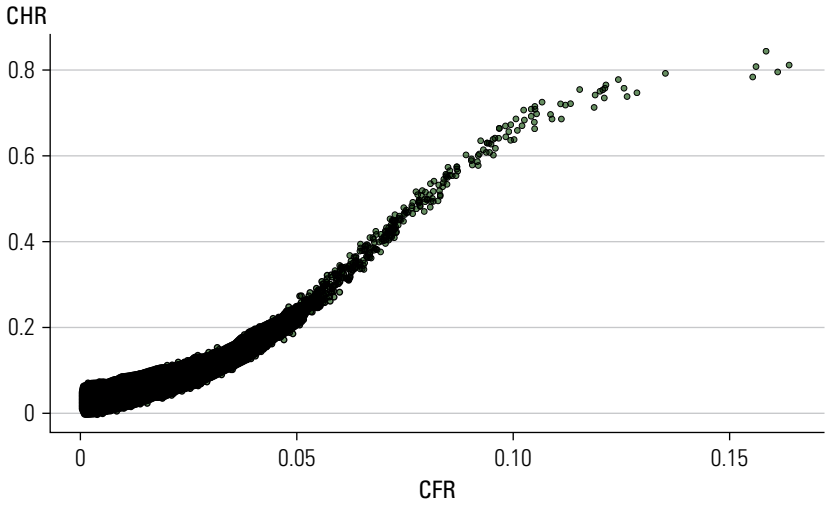

Source: Original figure created for this publication.

Spark Location

The location at which a zoonotic infectious disease emerges into human populations can affect the extent and severity of an epidemic. Respiratory epidemics can start anywhere in the world, but several factors can increase the risk of an area becoming a spark site. The likely location of epidemic emergence ("spark location") is modeled through geospatial analysis of environmental variables, animal host locations,

socioeconomic factors, and observed outbreak data. These data are formulated into emergence risk maps to identify high risk areas. This method often reveals areas of risk where cases have never been historically reported. The analyses performed are comparable to published works related to emergence mapping (Messina et al. 2016), such as for avian influenza and coronavirus spillover risk (Anthony et al. 2017; Dhingra et al. 2016; Sikkema et al. 2019).

Spark probabilities by country were estimated separately for pandemic influenza, MERS-like coronaviruses, and SARS-like coronaviruses (tables 2A.6, 2A.7, and 2A.8); estimates were aggregated up to regional groupings of countries. For all three categories, Asia and Africa had the greatest spark risk. For MERS-like coronaviruses, over 90 percent of the risk was concentrated in Asia, largely driven by high probabilities in the Middle East.

Table 2A.6 Proportion of Spark Risk for Pandemic Influenza Viruses, by Region

Region	Probability (%)
Asia	33.53
Africa	18.36
North America	17.20
South America	13.09
Europe	11.60
Oceania	6.22

Source: Original table created for this publication.

Note: Regions based on continental groupings.

Table 2A.7 Proportion of Spark Risk for MERS-Like Coronaviruses, by Region

Region	Probability (%)
Asia	92.92
Africa	5.42
Oceania	0.96
South America	0.32
North America	0.21
Europe	0.17

Source: Original table created for this publication

Note: Regions based on continental groupings. MERS = Middle East respiratory syndrome.

Table 2A.8 Proportion of Spark Risk for SARS-Like Coronaviruses, by Region

Region	Probability (%)
Asia	31.66
Africa	26.36
North America	14.71
Europe	13.78
South America	10.27
Oceania	3.21

Source: Original table created for this publication.

Note: Regions based on continental groupings. SARS = severe acute respiratory syndrome.

Event Frequency

Distributions of event frequency were developed from an analysis of historical data. Some types of events, such as MERS-like coronaviruses, typically have multiple occurrences per year, whereas less frequent events, such as pandemic influenza and SARS-like coronaviruses, would have, on average, less than one event per year (table 2A.9).

Table 2A.9 Parameterization of Event Frequency, by Pathogen Category

Pathogen category	Frequency distribution
Pandemic influenza (inter-arrival time, years)	Weibull (shape = 1.791395, scale = 33.63119) (min = 5, max = 135) (Morens et al. 2010)
MERS-like coronaviruses (events per quarter)	Truncated Negative Binomial (dispersion = 60, mu = 12, lower bound = 15) (min = 15, max = 26) (Eifan et al. 2017)
SARS-like coronaviruses (events per year)	Poisson (lambda = 0.1142857) (min = 0, max = 4) Analysis of Meadows et al. 2023 and Ginkgo Biosecurity data set[a]

Source: As indicated in the table.

Note: MERS = Middle East respiratory syndrome; SARS = severe acute respiratory syndrome.

a. Ginkgo Biosecurity, "Spatiotemporal Data for 2019-Novel Coronavirus Covid-19 Cases and Deaths," Humanitarian Data Exchange, https://data.humdata.org/dataset/2019-novel-coronavirus-cases.

Event Catalog Construction

The results presented in this chapter come from simulations for 100,000 years, representing 100,000 versions of "next year." The catalog size is determined by the number of simulations needed to achieve convergence in the tail risk estimates. Once the full set of stochastic simulations completes, it typically includes hundreds of thousands to millions of event scenarios, which are then compiled into an event catalog (Madhav, Stephenson, and Oppenheim 2021).

For each modeled event catalog, two versions were created. The first version is the Total Direct Catalog, which includes a full view of all spillover events and total case and death counts, not just those that are detected and reported. This catalog view allows for a more complete accounting of the true picture of loss. The second version is the Reported Catalog, which is adjusted for both the probability of detecting an event and the ratio at which cases and deaths are reported. This catalog version better reflects the realities of epidemic reporting and is more readily comparable to historical reported data. In keeping with the framework presented in the main text section on "Direct Deaths versus Excess Mortality," the estimates in the Reported Catalog represent Category D alone, whereas the Total Direct Catalog represents the sum of Categories C and D.

Exceedance Probability Functions

Once an event catalog has been created, it is used to develop a discretized exceedance probability function (EPF). This function results in estimates for the probability that an event of severity *s* or greater will occur in a given year. The EPF encapsulates two key factors, the frequency and severity of epidemics, into one function. This study uses deaths as the severity metric, though other measures of severity could be used (cases, economic losses, and so on). Specifically, the study used the annualized EPF. Annualization is achieved as such: if multiple epidemics occur in a simulated year, losses are aggregated by the year in which they start.

Operationally, the EPF is generated by sorting observation years in descending order and dividing the rank number by the total number of years in the event catalog. The simulated, discrete EPF is defined mathematically in the following way: Let S be a set of N independent severity observations having the members $\{S_1, S_2, S_3, \ldots, S_N\}$, where each S_j is the aggregation of losses beginning in each time period j. When the members of S are arranged in descending order, that is, the maximum S_j is first and the minimum S_j is last (in this example $(S_3 \geq S_1 \geq S_N \geq \ldots \geq S_2)$, and R_j is the rank number of the S_j observation (in this example, $R_3 = 1$, $R_1 = 2$, $R_N = 3$, …, $R_2 = N$), then the exceedance probability function of S_j is estimated as shown in equation (2A.2).

$$EPF\left(S_j\right) = \frac{R_j}{(N+1)} \qquad (2A.2)$$

Figure 2A.5 provides an example EPF plot.

Figure 2A.5 Example Exceedance Probability Function

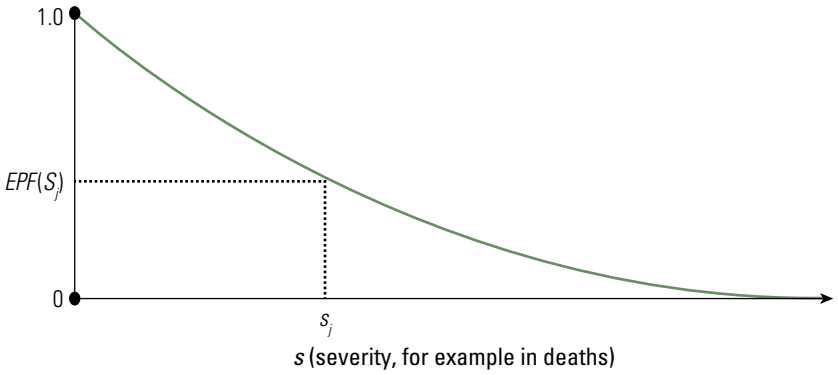

Source: Original figure created for this publication.

Note: EPF = exceedance probability function; *j* = time period; *S* = set of severity observations.

The inverse of EPF(s), r, is the return time (also known as return period or recurrence interval), shown in equation (2A.3).

$$r(s) = \frac{1}{EPF(s)} \tag{2A.3}$$

Some simulation years may have an equal number of deaths. To account for this scenario, equation (2A.4) gives the formulation of the discrete probability density function (*pdf*) associated with the EPF, where N is the number of simulation years and $n(s)$ is the number of simulation years resulting in severity s.

$$pdf(s) = \begin{cases} \frac{n(s)}{N} & if\ s \geq 0, \\ 0 & if\ s < 0. \end{cases} \tag{2A.4}$$

By probability theory, in the general case, the cumulative distribution function, $cdf(s)$ is defined by equation (2A.5).

$$cdf(s) = \int_{-\infty}^{s} pdf(x)dx \tag{2A.5}$$

The EPF is simply the complementary cumulative distribution function, as shown in equation (2A.6).

$$EPF(s) = 1 - cdf(s) \tag{2A.6}$$

Expected Value Calculation

A summary statistic of the EPF is the expected value (*EV*) of severity in a year, using the term expected value as it is used in probability theory. In extreme events modeling and insurance, it is known as the average annual loss (AAL). The AAL for an infectious disease event catalog is the mean number of cases, hospitalizations, deaths, or associated monetary loss across all simulation years in the event catalog. The value is highly skewed because of the inclusion of extreme events in the catalog. Additionally, for rare events, there are many years within the EPFs with low levels of deaths, punctuated by some years with very high numbers of deaths. The expected severity value of the discrete EPFs is given by equation (2A.7).

$$EV(EPF) = \sum\nolimits_{S} s \cdot pdf(s) \tag{2A.7}$$

In the continuous treatment, the expected value of the number of deaths for a given EPF is the area under the EPF curve, given by equation (2A.8).

$$EV(EPF) = \int_{0}^{\infty} EPF(s)ds \tag{2A.8}$$

Model Validation and Sensitivity Testing

Scenario inspection. A subset of scenarios were inspected to assess for biological and epidemiological plausibility. Table 2A.10 shows two different hypothetical scenarios simulated by the disease spread model. These events illustrate what potential scenarios might look like and are just two of thousands of example scenarios within the catalogs. The event magnitudes of 12 million and 80 million total global deaths (table 2A.11) were selected because they fall in different portions of the respiratory pathogen EPF. Events of this magnitude can take many forms, given the myriad of model parameters and the stochastic nature of the simulations. Notably, in both of these scenarios, the epidemic simmers at low levels of transmission before taking off and becoming a global pandemic (figure 2A.6).

Table 2A.10 Scenario Input Parameters

Parameter	Scenario 1	Scenario 2
Spark country	Canada	Türkiye
Incubation period (days)	3	5
R_0	1.679	1.716
Case fatality ratio	1.74%	4.54%
Case hospitalization ratio	6.64%	13.55%
Detection threshold	5 deaths	25 deaths
Timing of public health and social measures	30 days after detection in the spark country and 60 days after detection elsewhere	30 days after detection in the spark country and 60 days after detection elsewhere
R_t after interventions	0.9934	1.0502
Vaccination rate (proportion of population per day)	0.22% Varies by EPI	0.22% Varies by EPI
Vaccine efficacy	0.8	0.8
Vaccine proportion	0.7 Varies by EPI	0.7 Varies by EPI
Vaccine development time	326 days after detection Varies by EPI	326 days after detection Varies by EPI

Source: Original table created for this publication.

Note: EPI = Epidemic Preparedness Index.

Table 2A.11 Estimated Scenario Outcomes

Outcome	Scenario 1	Scenario 2
Infection counts (thousand)	686,000	1,800,000
Hospitalization counts (thousand)	47,000	249,000
Death counts (thousand)	12,300	83,300

Source: Ginkgo Biosecurity simulations.

Figure 2A.6 Simulated Epidemic Curves for Scenario 1 (12 Million Global Deaths) and Scenario 2 (80 Million Global Deaths)

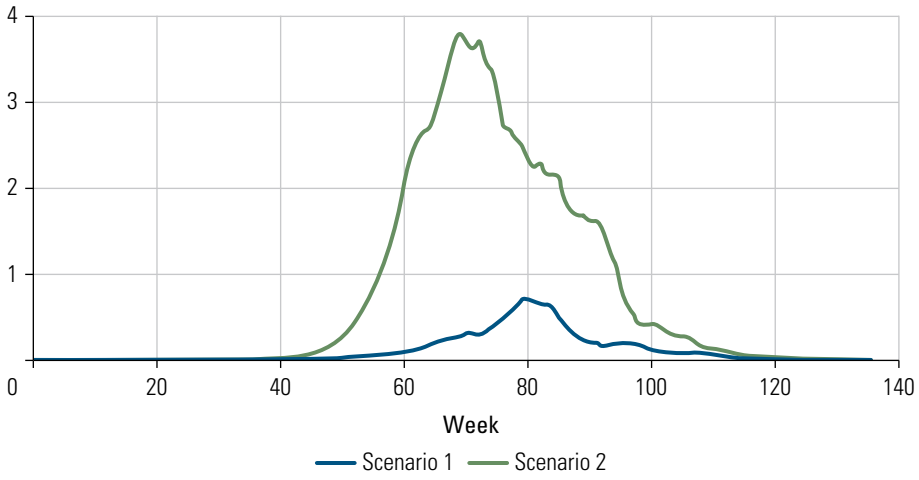

Source: Original figure created for this publication.

Sensitivity testing. Sensitivity analyses were performed to determine the response of the model to variations in parameter values. The analysis used the total number of infections as the output of interest. The analysis first required the simulation of a set of baseline scenarios. Then, additional simulations were produced by varying a single parameter around the baseline value while keeping all other parameters constant. This process was repeated for each model parameter. Table 2A.12 shows the list of parameters tested.

A sensitivity index based on partial rank correlation coefficients was calculated for each parameter and displayed in a tornado plot (figure 2A.7). Sensitivity indexes for vaccine-related, and nonvaccine parameters were run separately because a nonvaccine baseline scenario was used to test nonvaccine-related parameters.

The sensitivity analysis found that intervention timing, vaccine timing, and R_0 are strongly influential parameters in the overall simulated outbreak size. Incubation period is moderately influential, and the remaining parameters are only mildly influential. These findings are consistent with what is expected based on manual inspection of model output, basic epidemiological principles, and what is found in the literature for similar models.

Table 2A.12 Sensitivity Testing Results Demonstrated by Partial Rank Correlation Coefficients

Parameter	Original	Bias	Standard error	Lower 95% CI	Upper 95% CI
R_0	0.4053	0.0020	0.0342	0.3376	0.4729
Intervention time	0.0018	–0.0002	0.0397	–0.0806	0.0785
Incubation period	–0.0866	0.0002	0.0397	–0.1637	–0.0107
Intervention R_t	0.1794	0.0005	0.0391	0.1048	0.2525
Vaccine efficacy	0.0572	–0.0012	0.0393	–0.0139	0.1393
Vaccine start day	–0.0492	0.0002	0.0408	–0.1280	0.0316
Vaccine proportion	0.0264	–0.0010	0.0407	–0.0513	0.1059

Source: Original table created for this publication.

Note: CI = confidence interval.

Figure 2A.7 Graphical Depiction of Sensitivity Testing Results

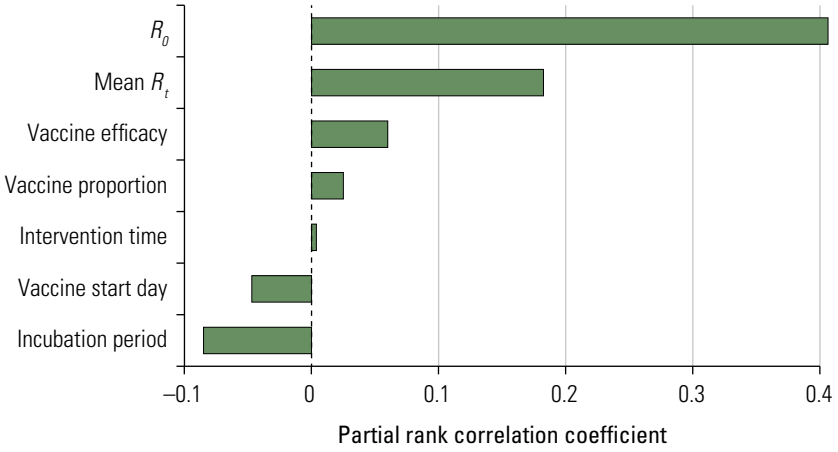

Source: Original figure created for this publication.

Historical event comparison. Testing of the disease spread model was conducted to assess for concordance of model results with historical events. Simulated pandemics used parameter values similar to those reported in the scientific literature for historical events, including prior influenza and coronavirus pandemics. The 2009 influenza pandemic and COVID-19 occurred in a world that bears a closer resemblance to the world modeled here, and the inherent assumptions (for example, population structure, mobility patterns, medical countermeasures) are more applicable than for earlier pandemics.

For the 2009 influenza pandemic, the modeled mortality estimates were compared to historical estimates found in the scientific literature (Dawood et al. 2012). Results are shown in figure 2A.8. Given the probabilistic nature of confidence intervals, it is expected that some model estimates would fall outside of the ranges recorded, and this was found to be the case particularly for lower-income countries. This result may be due to incomplete surveillance of influenza-related mortality in those locations.

Figure 2A.8 Comparison of Modeled Influenza-Related Deaths to Historical Estimates for the 2009 Influenza Pandemic, Selected Countries

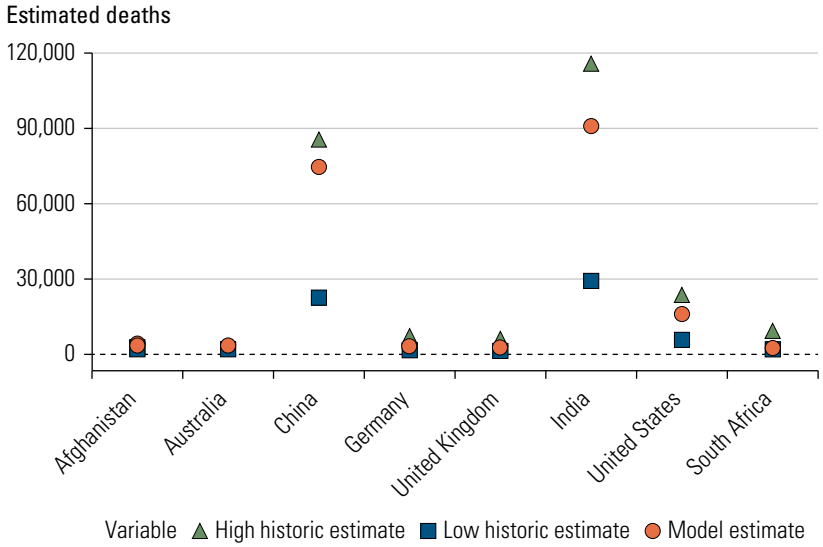

Source: Original figure created for this publication, based on Ginkgo Biosecurity simulations (circles) and historical estimates from Dawood et al. 2012 (triangles and squares).

To assess the temporal progression of the 2009-like pandemic simulation, the timing of the modeled peak incidence was compared to historical event data (Archer et al. 2009; CDC 2010; Choudhry et al. 2012; Echevarría-Zuno et al. 2009; Merler et al. 2011; Oliveira et al. 2009; Tizzoni et al. 2012).[3] This comparison found that the timing of the modeled peak incidence for the 2009 pandemic showed good agreement with historical data (figure 2A.9). During this simulation, most countries experienced their highest number of symptomatic cases within a few weeks of historic estimates, suggesting that the human mobility network and disease transmission processes within the model portray rates of disease spread in a realistic fashion. The slight delay from the model could result from assumptions on the spark timing of the event, transmissibility reduction due to seasonality, or temporal biases in case ascertainment.

Results from a model fitting and comparison exercise performed for the COVID-19 pandemic are reported elsewhere (Oppenheim et al., forthcoming; United Nations 2021). This comparison showed reasonable agreement of event trajectory and magnitude of estimates between modeled and historical data.

Figure 2A.9 Week of Peak Symptomatic Cases, 2009 Influenza Pandemic

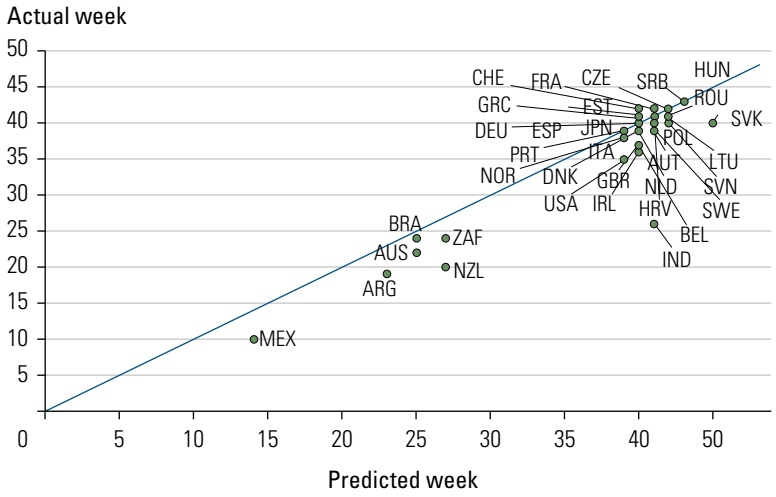

Source: Original figure created for this publication, based on Ginkgo Biosecurity simulations and historical event data from Archer et al. 2009; CDC 2010; Choudhry et al. 2012; Echevarría-Zuno et al. 2009; Merler et al. 2011; Oliveira et al. 2009; Tizzoni et al. 2012.

Note: Three-digit codes are ISO3 country codes.

Historical benchmarking. Policy makers and planners also benchmark modeled losses against historical experience. Table 2A.13 shows estimated EPs of historical events based on the modeled EPF to estimate these events' contemporary probability of occurrence. This analysis used reported mortality data from notable historical epidemics, estimated the proportion of the global population these deaths represented at the time of the event, and then calculated the number of deaths that the same proportion would represent for the 2020 global population (UN DESA 2022). The mortality estimate for each event was then used in conjunction with the EPF to estimate the EP value and extrapolated to the 10-year cumulative EP (CEP) based on the formula provided in the main text.

For historical benchmarking, unlike most of the estimates presented elsewhere in this chapter and supplementary materials, the analysis used the modeled Reported Catalog, rather than the Total Direct Catalog. This approach was used for historical benchmarking because historically reported information is more directly comparable to the Reported Catalog than to the Total Direct Catalog.

Table 2A.13 Estimated Exceedance Probabilities for Notable Historical Respiratory Epidemics and Pandemics

Event (years)	Global reported deaths (thousand) (Madhav et al. 2017)	Global reported deaths, adjusted to 2020 population (thousand)	Global reported deaths (% mortality)	Annual EP (%)	10-year EP (%)
SARS (2003)	0.774	0.944	0.00001	8–9	57–61
COVID-19 (2019–22)	6,500	6,500	0.08	2–3	18–26
1957 influenza pandemic (1957–58)	700–1,500	1,872–3,978	0.02–0.05	3.5–5.0	30–40
1968 influenza pandemic (1968–70)	1,000	2,184	0.03	4.4–4.8	36–39
2009 influenza pandemic (2009–10)	152–576	156–624	0.002–0.010	6–7	46–52
1918 influenza pandemic (1918–20)	20,000–100,000	86,580–432,900	1.11–5.55	< 0.001	< 1

Source: Original table created for this publication.

Note: EP = exceedance probability; SARS = severe acute respiratory syndrome. The COVID-19 global reported deaths is not from Madhav et al. 2017, but rather is based on data from Ginkgo Biosecurity, "Global Spatiotemporal Data for 2019-Novel Coronavirus Covid-19 Cases and Deaths," Humanitarian Data Exchange, https://data.humdata.org/dataset/2019-novel-coronavirus-cases.

ANNEX 2B. COUNTRY AND REGIONAL GROUPINGS

Table 2B.1 Country Regional Groupings

Central and Eastern Europe	Central Asia	China	India	Latin America and the Caribbean	Middle East and North Africa	North Atlantic	Sub-Saharan Africa	United States	Western Pacific and Southeast Asia
Albania	Afghanistan			Argentina	Algeria	Austria	Angola		Australia
Armenia	Azerbaijan			Bahamas, The	Bahrain	Belgium	Benin		Bangladesh
Belarus	Kazakhstan			Belize	Egypt, Arab Rep.	Canada	Botswana		Bhutan
Bosnia and Herzegovina	Kyrgyz Republic			Bolivia	Iran, Islamic Rep.	Cyprus	Burkina Faso		Brunei Darussalam
Bulgaria	Mongolia			Brazil	Iraq	Denmark	Burundi		Cambodia
Croatia	Pakistan			Chile	Israel	Finland	Cabo Verde		Fiji
Czech Republic	Tajikistan			Colombia	Jordan	France	Cameroon		Indonesia
Estonia	Turkmenistan			Costa Rica	Kuwait	Germany	Central African Republic		Japan
Georgia	Uzbekistan			Cuba	Lebanon	Greece	Chad		Korea, Dem. People's Rep.
Hungary				Dominican Republic	Libya	Iceland	Comoros		Korea, Rep.
Latvia				Ecuador	Morocco	Ireland	Congo, Dem. Rep.		Lao PDR
Lithuania				El Salvador	Oman	Italy	Congo, Rep.		Malaysia
Moldova				Guatemala	Qatar	Luxembourg	Côte d'Ivoire		Maldives
Montenegro				Guyana	Saudi Arabia	Malta	Djibouti		Myanmar

table continues next page

Table 2B.1 Country Regional Groupings (continued)

Central and Eastern Europe	Central Asia	China	India	Latin America and the Caribbean	Middle East and North Africa	North Atlantic	Sub-Saharan Africa	United States	Western Pacific and Southeast Asia
North Macedonia				Haiti	Syrian Arab Republic	Netherlands	Equatorial Guinea		Nepal
Poland				Honduras	Tunisia	Norway	Eritrea		New Zealand
Romania				Jamaica	Türkiye	Portugal	Eswatini		Papua New Guinea
Russian Federation				Mexico	United Arab Emirates	Spain	Ethiopia		Philippines
Serbia				Nicaragua	Yemen, Rep.	Sweden	Gabon		Singapore
Slovak Republic				Panama		Switzerland	Gambia, The		Solomon Islands
Slovenia				Paraguay		United Kingdom	Ghana		Sri Lanka
Ukraine				Peru			Guinea		Thailand
				Suriname			Guinea-Bissau		Timor-Leste
				Trinidad and Tobago			Kenya		Vanuatu
				Uruguay			Lesotho		Viet Nam
				Venezuela, RB			Liberia		
							Madagascar		
							Malawi		
							Mali		
							Mauritania		
							Mauritius		
							Mozambique		
							Namibia		
							Niger		
							Nigeria		
							Rwanda		
							Senegal		
							Sierra Leone		
							Somalia		
							South Africa		
							South Sudan		
							Sudan		
							Tanzania		
							Togo		
							Uganda		
							Zambia		
							Zimbabwe		

Source: Disease Control Priorities 4 Secretariat.

ANNEX 2C. SENSITIVITY ANALYSIS FOR CHANGES IN FREQUENCY/ SEVERITY ASSUMPTIONS

Because the estimates for the 5-, 10-, and 25-year cumulative exceedance probabilities (CEPs) did not assume any trend, and because of the great uncertainty in that assumption, a sensitivity analysis on this assumption was performed. For the sensitivity analysis, plausible values that trends in the frequency and severity of diseases may exhibit over time were selected. These values ranged from a 2 percent year-over-year decrease to a 5 percent year-over-year increase. The analysis kept the value of no annual trend, to correspond to the estimates shown in the main text. The trend assumptions were applied using the formula,

$$CEP(N,T) = 1 - \left((1 - AEP) \times \prod_{i=1}^{N-1} (1+T)^i \right),$$

where *CEP* is the cumulative exceedance probability, *N* is the number of years, *T* is the trend assumption, and *AEP* is the annualized exceedance probability.

Results are shown in table 2C.1 and indicate that the CEP is less sensitive to this assumption at shorter time horizons but can be sensitive at longer time horizons. Estimates that are further out in the tail are also more sensitive to the assumptions. Table 2C.2 presents results for a similar analysis performed for VHF in Sub-Saharan Africa.

Table 2C.1 Five-Year, 10-Year, and 25-Year Cumulative Exceedance Probability Estimates for Selected Global Event Sizes Based on the Respiratory Event Catalog, with Varying Annual Trend Assumptions

Deaths	2% annual decrease (%)	1% annual decrease (%)	No annual trend (%)	3% annual increase (%)	5% annual increase (%)
5-year cumulative exceedance probability					
1,000,000	27	27	28	29	30
10,000,000	18	19	19	20	21
25,000,000	12	12	12	13	13
100,000,000	2.9	3.0	3.0	3.2	3.4
10-year cumulative exceedance probability					
1,000,000	45	46	48	53	56
10,000,000	32	33	35	39	42
25,000,000	21	22	23	26	28
100,000,000	5.5	5.7	5.8	6.9	7.5
25-year cumulative exceedance probability					
1,000,000	72	76	80	91	96
10,000,000	57	61	66	79	88
25,000,000	40	44	48	61	72
100,000,000	12	13	14	20	26

Source: Ginkgo Biosecurity simulations.

Table 2C.2 Five-Year, 10-Year, and 25-Year Cumulative Exceedance Probability Estimates for Selected Sub-Saharan Africa Event Sizes Based on the VHF Event Catalog, with Varying Annual Trend Assumptions

Deaths	2% annual decrease (%)	1% annual decrease (%)	No annual trend (%)	3% annual increase (%)	5% annual increase (%)
5-year cumulative exceedance probability					
10,000	33	34	34	36	37
50,000	16	17	17	18	19
100,000	12	12	12	13	13
10-year cumulative exceedance probability					
10,000	54	55	57	62	66
50,000	29	30	31	35	38
100,000	21	22	23	26	28
25-year cumulative exceedance probability					
10,000	81	85	88	96	99
50,000	52	56	61	75	84
100,000	40	44	48	61	71

Source: Ginkgo Biosecurity simulations.

Note: VHF = viral hemorrhagic fever.

NOTES

The authors gratefully acknowledge the University of Bergen Centre for Ethics and Priority Setting in Health and the Norwegian Agency for Development Cooperation (NORAD) (RAF-18/0009) for providing funding support. Certain supporting data and code are publicly available in the following repositories:

- Zoonotic disease data: https://github.com/concentricbyginkgo/zoonotic_spillover_trend
- Underreporting: https://github.com/metabiota-ameadows/underreporting
- COVID-19 data set: https://data.humdata.org/dataset/2019-novel-coronavirus-cases.

Other data and model code are considered commercial/proprietary and cannot be publicly released. Nita K. Madhav, Ben Oppenheim, Nicole Stephenson, Rinette Badker, Cathine Lam, and Amanda Meadows are or have been employed by Ginkgo Bioworks.

1. MERS-CoV refers to Middle East respiratory syndrome coronavirus, SARS-CoV-1 refers to the severe acute respiratory coronavirus responsible for the 2002–04 SARS outbreak, and SARS-CoV-2 refers to the coronavirus that causes COVID-19.
2. OAG, "Global Airline Schedules Data," https://www.oag.com/airline-schedules-data.
3. Infectious Disease Surveillance Center, Japan, "Influenza cases reported per sentinel weekly, 2002–2012, http://idsc.nih.go.jp/idwr/kanja/weeklygraph/01flu-e.html.

REFERENCES

Adam, D. C., P. Wu, J. Y. Wong, E. H. Y. Lau, T. K. Tsang, S. Cauchemez, G. M. Leung, and B. J. Cowling. 2020. "Clustering and Superspreading Potential of SARS-CoV-2 Infections in Hong Kong." *Nature Medicine* 26: 1714–19.

Alene, M., L. Yismaw, M. A. Assemie, D. B. Ketema, W. Gietaneh, and T. Y. Birhan. 2021. "Serial Interval and Incubation Period of COVID-19: A Systematic Review and Meta-analysis." *BMC Infectious Diseases* 21: 1–9.

Ali, S. T., L. Wang, E. H. Y. Lau, X.-K. Xu, Z. Du, Y. Wu, G. M. Leung, and B. J. Cowling. 2020. "Serial Interval of SARS-CoV-2 Was Shortened over Time by Nonpharmaceutical Interventions." *Science* 369 (6507): 1106–9.

Andreasen, V., C. Viboud, and L. Simonsen. 2008. "Epidemiologic Characterization of the 1918 Influenza Pandemic Summer Wave in Copenhagen: Implications for Pandemic Control Strategies." *The Journal of Infectious Diseases* 197 (2): 270–78.

Angulo, F. J., L. Finelli, and D. L. Swerdlow. 2021. "Estimation of US SARS-CoV-2 Infections, Symptomatic Infections, Hospitalizations, and Deaths Using Seroprevalence Surveys." *JAMA Network Open* 4 (1): e2033706.

Anthony, S. J., C. K. Johnson, D. J. Greig, S. Kramer, X. Che, H. Wells, A. L. Hicks, et al. 2017. "Global Patterns in Coronavirus Diversity." *Virus Evolution* 3 (1): vex012.

Archer, B. N., C. Cohen, D. Naidoo, J. Thomas, C. Makunga, L. Blumberg, M. Venter, et al. 2009. "Interim Report on Pandemic H1N1 Influenza Virus Infections in South Africa, April to October 2009: Epidemiology and Factors Associated with Fatal Cases." *Eurosurveillance* 14 (42): 19369.

Balcan, D., V. Colizza, B. Gonçalves, H. Hu, J. J. Ramasco, and A. Vespignani. 2009. "Multiscale Mobility Networks and the Spatial Spreading of Infectious Diseases." *Proceedings of the National Academy of Sciences of the United States of America* 106 (51): 21484–89.

Bo, Y., C. Guo, C. Lin, Y. Zeng, H. B. Li, Y. Zhang, M. S. Hossain, et al. 2021. "Effectiveness of Non-pharmaceutical Interventions on COVID-19 Transmission in 190 Countries from 23 January to 13 April 2020." *International Journal of Infectious Diseases* 102: 247–53.

Breban, R., J. Riou, and A. Fontanet. 2013. "Interhuman Transmissibility of Middle East Respiratory Syndrome Coronavirus: Estimation of Pandemic Risk." *The Lancet* 382 (9893): 694–99.

Britten, R. H. 1932. "The Incidence of Pandemic Influenza, 1918–19: A Further Analysis According to Age, Sex, and Color of the Records of Morbidity and Mortality Obtained in Surveys of 12 Localities." *Public Health Reports* 47 (6): 303–75.

Carrat, F., E. Vergu, N. M. Ferguson, M. Lemaitre, S. Cauchemez, S. Leach, and A.-J. Valleron. 2008. "Time Lines of Infection and Disease in Human Influenza: A Review of Volunteer Challenge Studies." *American Journal of Epidemiology* 167 (7): 775–85.

Cauchemez, S., C. Fraser, M. D. Van Kerkhove, C. A. Donnelly, S. Riley, A. Rambaut, V. Enouf, et al. 2014. "Middle East Respiratory Syndrome Coronavirus: Quantification of the Extent of the Epidemic, Surveillance Biases, and Transmissibility." *The Lancet Infectious Diseases* 14 (1): 50–56.

CDC (Centers for Disease Control and Prevention). 2010. Update: Influenza Activity–United States, 2009–10 Season." *Morbidity and Mortality Weekly Report* 59 (29): 901–8.

Chan, E. H., T. F. Brewer, L. C. Madoff, M. P. Pollack, A. L. Sonricker, M. Keller, C. C. Freifeld, et al. 2010. "Global Capacity for Emerging Infectious Disease Detection." *Proceedings of the National Academy of Sciences of the United States of America* 107 (50): 21701–6.

Choe, S., H.-S. Kim, and S. Lee. 2020. "Exploration of Superspreading Events in 2015 MERS-CoV Outbreak in Korea by Branching Process Models." *International Journal of Environmental Research and Public Health* 17 (17): 6137.

Choudhry, A., S. Singh, S. Khare, A. Rai, D. S. Rawat, R. K. Aggarwal, amd L. S. Chauhan. 2012. "Emergence of Pandemic 2009 Influenza A H1N1, India." *The Indian Journal of Medical Research* 135 (4): 534.

Chowell, G., F. Abdirizak, S. Lee, J. Lee, E. Jung, H. Nishiura, and C. Viboud. 2015. "Transmission Characteristics of MERS and SARS in the Healthcare Setting: A Comparative Study." *BMC Medicine* 13 (1): 210.

Chowell, G., C. Castillo-Chavez, P. W. Fenimore, C. M. Kribs-Zaleta, L. Arriola, and J. M. Hyman. 2004. "Model Parameters and Outbreak Control for SARS." *Emerging Infectious Diseases* 10 (7): 1258–63.

Chowell, G., S. Echevarría-Zuno, C. Viboud, L. Simonsen, J. Tamerius, M. A. Miller, and V. H. Borja-Aburto. 2011. "Characterizing the Epidemiology of the 2009 Influenza A/H1N1 Pandemic in Mexico." *PLOS Medicine* 8 (5): e1000436.

Colizza, V., A. Barrat, M. Barthelemy, A.-J. Valleron, and A. Vespignani. 2007. "Modeling the Worldwide Spread of Pandemic Influenza: Baseline Case and Containment Interventions." *PLOS Medicine* 4 (1): e13.

Dalziel, B. D., M. S. Y. Lau, A. Tiffany, A. McClelland, J. Zelner, J. R. Bliss, and B. T. Grenfell. 2018. "Unreported Cases in the 2014-2016 Ebola Epidemic: Spatiotemporal Variation, and Implications for Estimating Transmission." *PLOS Neglected Tropical Diseases* 12 (1): e0006161.

Dawood, F. S., A. D. Iuliano, C. Reed, M. I. Meltzer, D. K. Shay, P.-Y. Cheng, D. Bandaranayake, et al. 2012. "Estimated Global Mortality Associated with the First 12 Months of 2009 Pandemic Influenza A H1N1 Virus Circulation: A Modelling Study." *The Lancet Infectious Diseases* 12 (9): 687–95.

Dhingra, M. S., J. Artois, T. P. Robinson, C. Linard, C. Chaiban, I. Xenarios, R. Engler, et al. 2016. "Global Mapping of Highly Pathogenic Avian Influenza H5N1 and H5Nx Clade 2.3.4.4 Viruses with Spatial Cross-Validation." *ELife* 5: e19571.

Echevarría-Zuno, S., J. M. Mejía-Aranguré, A. J. Mar-Obeso, C. Grajales-Muñiz, E. Robles-Pérez, M. González-León, M. C. Ortega-Alvarez, et al. 2009. "Infection and Death from Influenza A H1N1 Virus in Mexico: A Retrospective Analysis." *The Lancet* 374 (9707): 2072–79.

Eifan, S. A., I. Nour, A. Hanif, A. M. M. Zamzam, and S. M. AlJohani. 2017. "A Pandemic Risk Assessment of Middle East Respiratory Syndrome Coronavirus (MERS-CoV) in Saudi Arabia." *Saudi Journal of Biological Sciences* 24 (7): 1631–38.

Gamado, K., G. Streftaris, and S. Zachary. 2017. "Estimation of Under-Reporting in Epidemics Using Approximations." *Journal of Mathematical Biology* 74 (7): 1683–707.

Gani, R., H. Hughes, D. Fleming, T. Griffin, J. Medlock, and S. Leach. 2005. "Potential Impact of Antiviral Drug Use during Influenza Pandemic." *Emerging Infectious Diseases* 11 (9): 1355–62.

Graña, C., L. Ghosn, T. Evrenoglou, A. Jarde, S. Minozzi, H. Bergman, B. S. Buckley, et al. 2023. "Efficacy and Safety of COVID-19 Vaccines." *Cochrane Database of Systematic Reviews* 12 (12): CD015477.

Grewelle, R. E., and G. A. D. Leo. 2020. *Estimating the Global Infection Fatality Rate of COVID-19*. https://www.medrxiv.org/content/10.1101/2020.05.11.20098780v1.

Henderson, D. A., B. Courtney, T. V. Inglesby, E. Toner, and J. B. Nuzzo. 2009. "Public Health and Medical Responses to the 1957-58 Influenza Pandemic." *Biosecurity and Bioterrorism: Biodefense Strategy, Practice, and Science* 7: (3): 265–73.

Hessel, L., and EVM (European Vaccine Manufacturers) Influenza Working Group. 2009. "Pandemic Influenza Vaccines: Meeting the Supply, Distribution and Deployment Challenges." *Influenza and Other Respiratory Viruses* 3 (4): 165–70.

Jackson, C., E. Vynnycky, and P. Mangtani. 2010. "Estimates of the Transmissibility of the 1968 (Hong Kong) Influenza Pandemic: Evidence of Increased Transmissibility between Successive Waves." *American Journal of Epidemiology* 171 (4): 465–78.

Jia, N., D. Feng, L. Fang, J. H. Richardus, X. Han, W. Cao, and S. J. De Vlas. 2009. "Case Fatality of SARS in Mainland China and Associated Risk Factors." *Tropical Medicine & International Health* 14 (s1): 21–27.

Kenyon, C. 2020. "COVID-19 Infection Fatality Rate Associated with Incidence—A Population-Level Analysis of 19 Spanish Autonomous Communities." *Biology* 9 (6): 128.

Lau, M. S. Y., B. Grenfell, M. Thomas, M. Bryan, K. Nelson, and B. Lopman. 2020. "Characterizing Superspreading Events and Age-Specific Infectiousness of SARS-CoV-2 Transmission in Georgia, USA." *Proceedings of the National Academy of Sciences* 117 (36): 22430–35.

Lee, V. J., C. S. Wong, P. A. Tambyah, J. Cutter, M. I. Chen, and K. T. Goh. 2008. "Twentieth Century Influenza Pandemics in Singapore." *Annals, Academy of Medicine, Singapore* 37 (6): 470.

Lessler, J., N. G. Reich, R. Brookmeyer, T. M. Perl, K. E. Nelson, and D. A. Cummings. 2009. "The Incubation Periods of Acute Respiratory Viral Infections: A Systematic Review." *The Lancet Infectious Diseases* 9 (5): 291–300.

Liang, W., M.-L. McLaws, M. Liu, J. Mi, and D. K. Y. Chan. 2007. "Hindsight: A Re-analysis of the Severe Acute Respiratory Syndrome Outbreak in Beijing." *Public Health* 121 (10): 725–33.

Lipsitch, M., T. Cohen, B. Cooper, J. M. Robins, S. Ma, L. James, G. Gopalakrishna, et al. 2003. "Transmission Dynamics and Control of Severe Acute Respiratory Syndrome." *Science* 300 (5627): 1966–70.

Liu, R., R. K. Leung, T. Chen, X. Zhang, F. Chen, S. Chen, and J. Zhao. 2015. "The Effectiveness of Age-Specific Isolation Policies on Epidemics of Influenza A (H1N1) in a Large City in Central South China." *PLOS One* 10 (7): e0132588.

Longini, I. M., M. E. Halloran, A. Nizam, and Y. Yang. 2004. "Containing Pandemic Influenza with Antiviral Agents." *American Journal of Epidemiology* 159 (7): 623–33.

Longini, I. M., A. Nizam, S. Xu, K. Ungchusak, W. Hanshaoworakul, D. A. T. Cummings, and M. E. Halloran. 2005. "Containing Pandemic Influenza at the Source." *Science* 309 (5737): 1083–87.

Luo, G., X. Zhang, H. Zheng, and D. He. 2021. "Infection Fatality Ratio and Case Fatality Ratio of COVID-19." *International Journal of Infectious Diseases* 113 (December): 43–46.

Madhav, N., B. Oppenheim, M. Gallivan, P. Mulembakani, E. Rubin, and N. Wolfe. 2017. "Pandemics: Risks, Impacts, and Mitigation." In *Disease Control Priorities* (third edition), Volume 9, *Improving Health and Reducing Poverty*, edited by D. T. Jamison, H. Gelband, S. Horton, P. Jha, R. Laxminarayan, C. N. Mock, and R. Nugent. Washington, DC: World Bank. http://www.ncbi.nlm.nih.gov/books/NBK525302/.

Madhav, N., N. Stephenson, and B. Oppenheim. 2021. "Multipathogen Event Catalogs Technical Note." World Bank, Washington, DC. https://documents1.worldbank.org/curated/en/181791625232959415/pdf/Multi-Pathogen-Event-Catalogs-Technical-Note.pdf.

Majumder, M. S., C. Rivers, E. Lofgren, and D. Fisman. 2014. "Estimation of MERS-Coronavirus Reproductive Number and Case Fatality Rate for the Spring 2014 Saudi Arabia Outbreak: Insights from Publicly Available Data." *PLOS Currents Outbreaks*, December 18. https://pmc.ncbi.nlm.nih.gov/articles/PMC4322060.

Martinez, D. L., and T. K. Das. 2014. "Design of Non-pharmaceutical Intervention Strategies for Pandemic Influenza Outbreaks." *BMC Public Health* 14 (1): 1–14.

Mathieu, E., H. Ritchie, L. Rodés-Guirao, C. Appel, D. Gavrilov, C. Giattino, J. Hasell, et al. 2020. "Coronavirus (COVID-19) Vaccinations." *Our World in Data*. https://ourworldindata.org/covid-vaccinations.

McAloon, C., Á. Collins, K. Hunt, A. Barber, A. W. Byrne, F. Butler, M. Casey, et al. 2020. "Incubation Period of COVID-19: A Rapid Systematic Review and Meta-analysis of Observational Research." *BMJ Open* 10 (8): e039652.

Meadows, A. J., B. Oppenheim, J. Guerrero, B, Ash, R. Badker, C. K. Lam, C. Pardee, et al. 2022. "Infectious Disease Underreporting Is Predicted by Country-Level Preparedness, Politics, and Pathogen Severity." *Health Security* 20 (4): 331–38.

Meadows, A. J., N. Stephenson, N. K. Madhav, and B. Oppenheim. 2023. "Historical Trends Demonstrate a Pattern of Increasingly Frequent and Severe Epidemics of High-Consequence Zoonotic Viruses." *BMJ Global Health* 8 (11): e012026.

Merler, S., M. Ajelli, A. Pugliese, and N. M. Ferguson. 2011. "Determinants of the Spatiotemporal Dynamics of the 2009 H1N1 Pandemic in Europe: Implications for Real-Time Modelling." *PLOS Computational Biology* 7 (9): e1002205.

Messina, J. P., M. U. Kraemer, O. J. Brady, D. M. Pigott, F. M. Shearer, D. J. Weiss, N. Golding, et al. 2016. "Mapping Global Environmental Suitability for Zika Virus." *ELife* 5: e15272.

Mihigo, R., C. V. Torrealba, K. Coninx, D. Nshimirimana, M. P. Kieny, P. Carrasco, L. Hedman, and M.-A. Widdowson. 2012. "2009 Pandemic Influenza A Virus Subtype H1N1 Vaccination in Africa—Successes and Challenges." *The Journal of Infectious Diseases* 206 (suppl_1): S22–S28.

Morens, D. M., J. K. Taubenberger, G. K. Folkers, and A. S. Fauci. 2010. "Pandemic Influenza's 500th Anniversary." *Clinical Infectious Diseases* 51 (12): 1442–44.

Nichol, K. L., and J. J. Treanor. 2006. "Vaccines for Seasonal and Pandemic Influenza." *The Journal of Infectious Diseases* 194 (Supplement_2): S111–18.

Oliveira, W. K., E. H. Carmo, G. O. Penna, R. S. Kuchenbecker, H. B. Santos, W. N. Araújo, R. Malaguti, et al. 2009. "Pandemic H1N1 Influenza in Brazil: Analysis of the First 34,506 Notified Cases of Influenza-Like Illness with Severe Acute Respiratory Infection (SARI)." *Eurosurveillance* 14 (42): 19362.

Oppenheim, B., M. Gallivan, N. K. Madhav, N. Brown, V. Serhiyenko, N. D. Wolfe, and P. Ayscue. 2019. "Assessing Global Preparedness for the Next Pandemic: Development and Application of an Epidemic Preparedness Index." *BMJ Global Health* 4 (1): e001157.

Oppenheim, B., N. Stephenson, N. K. Madhav, D. T. Jamison, A. Alawan, K. Brown, G. Chowell, et al. Forthcoming. "The Value is in the Network: The Impact of Multilateral Cooperation on the COVID-19 Pandemic." Working paper.

Presanis, A. M., D. D. Angelis, A. Hagy, C. Reed, S. Riley, B. S. Cooper, L. Finelli, et al. 2009. "The Severity of Pandemic H1N1 Influenza in the United States, from April to July 2009: A Bayesian Analysis." *PLOS Medicine* 6 (12): e1000207.

Rivers, C. M., M. S. Majumder, and E. T. Lofgren. 2016. "Risks of Death and Severe Disease in Patients with Middle East Respiratory Syndrome Coronavirus, 2012–2015" *American Journal of Epidemiology* 184 (6): 460–64.

Rizzo, C., M. Ajelli, S. Merler, A. Pugliese, I. Barbetta, S. Salmaso, and P. Manfredi. 2011. "Epidemiology and Transmission Dynamics of the 1918–19 Pandemic Influenza in Florence, Italy." *Vaccine* 29 (s2): B27–B32.

Rvachev, L. A., and I. M. Longini. 1985. "A Mathematical Model for the Global Spread of Influenza." *Mathematical Biosciences* 75 (1): 3–22.

Shrestha, S. S., D. L. Swerdlow, R. H. Borse, V. S. Prabhu, L. Finelli, C. Y. Atkins, K. Owusu-Edusei, et al. 2011. "Estimating the Burden of 2009 Pandemic Influenza A (H1N1) in the United States (April 2009–April 2010)." *Clinical Infectious Diseases* 52 (s1): S75–S82.

Shubin, M., M. Virtanen, S. Toikkanen, O. Lyytikäinen, and K. Auranen. 2014. "Estimating the Burden of A(H1N1)pdm09 Influenza in Finland during Two Seasons." *Epidemiology and Infection* 142 (5): 964–74.

Sikkema, R. S., E. A. B. A. Farag, M. Islam, M. Atta, C. B. E. M. Reusken, M. M. Al-Hajri, and M. P. G. Koopmans. 2019. "Global Status of Middle East Respiratory Syndrome Coronavirus in Dromedary Camels: A Systematic Review. *Epidemiology and Infection* 147: e84.

Tai, W., X. Zhang, Y. Yang, J. Zhu, and L. Du. 2022. "Advances in mRNA and Other Vaccines against MERS-CoV." *Translational Research* 242: 20–37.

Tizzoni, M., P. Bajardi, C. Poletto, J. J. Ramasco, D. Balcan, B. Gonçalves, N. Perra, et al. 2012. "Real-Time Numerical Forecast of Global Epidemic Spreading: Case Study of 2009 A/H1N1pdm." *BMC Medicine* 10 (1): 165.

Tuite, A. R., A. L. Greer, M. Whelan, A.-L. Winter, B. Lee, P. Yan, J. Wu, et al. 2010. "Estimated Epidemiologic Parameters and Morbidity Associated with Pandemic H1N1 Influenza." *Canadian Medical Association Journal* 182 (2): 131–36.

UN DESA (United Nations Department of Economic and Social Affairs). 2015. "World Population Prospects: The 2015 Revision, Key Findings and Advance Tables." United Nations, New York.

UN DESA (United Nations Department of Economic and Social Affairs). 2022. "World Population Prospects 2022: Data Sources." UN DESA/POP/2022/DC/NO. 9, United Nations, New York. https://www.un.org/development/desa/pd/sites/www.un.org.development.desa.pd/files/undesa_pd_2022_wpp-data_sources.pdf.

United Nations. 2021. *Our Common Agenda – Report of the Secretary-General*. New York: United Nations.

Valleron, A.-J., A. Cori, S. Valtat, S. Meurisse, F. Carrat, and P.-Y. Boëlle. 2010. "Transmissibility and Geographic Spread of the 1889 Influenza Pandemic." *Proceedings of the National Academy of Sciences of the United States of America* 107 (19): 8778–81.

White, L. F., and M. Pagano. 2008. "Transmissibility of the Influenza Virus in the 1918 Pandemic." *PLOS One* 3 (1): e1498.

White, L. F., J. Wallinga L. Finelli, C. Reed, S. Riley, M. Lipsitch, and M. Pagano. 2009. "Estimation of the Reproductive Number and the Serial Interval in Early Phase of the 2009 Influenza A/H1N1 Pandemic in the USA." *Influenza and Other Respiratory Viruses* 3 (6): 267–76.

WHO (World Health Organization). 2009. "Transmission Dynamics and Impact of Pandemic Influenza A (H1N1) 2009 Virus. *Weekly Epidemiological Record* 84 (46): 481–84.

WHO (World Health Organization). 2013. "Global Survey on National Vaccine Deployment and Vaccination Plans for Pandemic A(H1N1) 2009 Vaccine – 2010." WHO, Geneva.

Wong, J. Y., H. Kelly, D. K. M. Ip, J. T. Wu, G. M. Leung, and B. J. Cowling. 2013. "Case Fatality Risk of Influenza A(H1N1pdm09): A Systematic Review." *Epidemiology* 24 (6): 830–41.

Wu, J. T., E. S. K. Ma, C. K. Lee, D. K. W. Chu, P.-L. Ho, A. L. Shen, A. Ho, et al. 2010. "The Infection Attack Rate and Severity of 2009 Pandemic H1N1 Influenza in Hong Kong." *Clinical Infectious Diseases* 51 (10): 1184–91.

Wu, J. T., S. Riley, C. Fraser, and G. M. Leung. 2006. "Reducing the Impact of the Next Influenza Pandemic Using Household-Based Public Health Interventions." *PLOS Medicine* 3 (9): e361.

Yang, Y., J. D. Sugimoto, M. E. Halloran, N. E. Basta, D. L. Chao, L. Matrajt, G. Potter, E. Kenah, and I. M. Longini. 2009. "The Transmissibility and Control of Pandemic Influenza A (H1N1) Virus." *Science* 326 (5953): 729–33.

Zhang, S., P. Yan, B. Winchester, and J. Wang. 2009. "Transmissibility of the 1918 Pandemic Influenza in Montreal and Winnipeg of Canada." *Influenza and Other Respiratory Viruses* 4 (1): 27–31.